



1     **How does the OH reactivity affect the ozone production efficiency:**  
2  
3                                   **case studies in Beijing and Heshan**

4                   Yudong Yang<sup>1</sup>, Min Shao<sup>1</sup>\*, Stephan. Keßel<sup>2</sup>, Yue Li<sup>1</sup>, Keding Lu<sup>1</sup>, Sihua Lu<sup>1</sup>,  
5                   Jonathan Williams<sup>2</sup>, Yuanhang Zhang<sup>1</sup>, Liming Zeng<sup>1</sup>, Anke C. Nölscher<sup>2, #</sup>,  
6                   Yusheng Wu<sup>1</sup>, Xuemei Wang<sup>3</sup>, Junyu Zheng<sup>4</sup>,

7  
8     <sup>1</sup> State Joint Key Laboratory of Environmental Simulation and Pollution Control, College of  
9     Environmental Science and Engineering, Peking University, Beijing, China

10    <sup>2</sup> Department of Atmospheric Chemistry, Max Plank-Institute for Chemistry, Mainz, Germany

11    <sup>3</sup> School of Atmospheric Science, Sun Yat-Sen University, Guangzhou, China

12    <sup>4</sup> School of Environmental Science and Engineering, South China University of Technology, China

13    # now at: Division of Geological and Planetary Sciences, California Institute of Technology,  
14    Pasadena, USA

15  
16    \* Corresponding to: Min Shao

17    Email address: [mshao@pku.edu.cn](mailto:mshao@pku.edu.cn)

18  
19    **Abstract**

20           Total OH reactivity measurements have been conducted in August 2013 on the  
21    Peking University campus, Beijing and from October to November 2014 in Heshan,  
22    Guangdong Province. The daily median result for OH reactivity was  $19.98 \pm 11.03 \text{ s}^{-1}$   
23    in Beijing and  $30.62 \pm 19.76 \text{ s}^{-1}$  in Heshan. Beijing presented a significant diurnal  
24    variation with maxima over  $27 \text{ s}^{-1}$  in the early morning and minima below  $16 \text{ s}^{-1}$  in the  
25    afternoon. Measurements in Heshan gave a much flatter diurnal pattern. Missing  
26    reactivity was observed at both sites, with 21% missing in Beijing and 32% missing in  
27    Heshan. Unmeasured primary species, such as branched-alkenes could contribute to  
28    missing reactivity in Beijing, especially in morning rush hour. An observation-based  
29    model with the Regional Atmospheric Chemical Mechanism 2 was used to understand  
30    the daytime missing reactivity in Beijing by adding unmeasured oxygenated volatile  
31    organic compounds and simulated intermediates of primary VOCs degradation.  
32    However, the model failed to explain the missing reactivity in Heshan, where the  
33    ambient air was found to be more aged, and the missing reactivity was presumably to



34 attribute to oxidized species, such as aldehydes, acids and di-carbonyls. The ozone  
35 production efficiency was 27% higher in Beijing and 35% higher in Heshan when  
36 constrained by the measured reactivity, compared to the calculation with measured and  
37 modeled species included, indicating the importance of quantifying the OH reactivity  
38 for better understanding ozone chemistry.

39

## 40 1. Introduction

41 Studies on total OH reactivity in the atmosphere have been increasing over the last  
42 two decades. The instantaneous total OH reactivity, is defined as

$$43 \quad k_{OH} = \sum_i k_{OH+X_i}[x_i] \quad (1-1)$$

44 where X represents a reactive species (CO, NO<sub>2</sub> etc.) and  $k_{OH+X_i}$  is the rate  
45 coefficient for the reaction between X and OH radicals. Total OH reactivity is an  
46 effective index for evaluating the amounts of reductive pollutants in terms of ambient  
47 OH loss and hence their role in atmospheric oxidation (Williams, 2008; Williams and  
48 Brune, 2015; Yang et al., 2016). It also provides a constraint for OH budget researches  
49 in both field campaigns and lab studies (Stone et al., 2012; Fuchs et al., 2013).

50 There are three major total OH reactivity measuring techniques, two laser-  
51 induced-fluorescence (LIF) based techniques (Calpini, et al., 1999; Kovacs and Brune,  
52 2001) and one proton-transfer-reaction mass spectrometry (PTR-MS) based technique,  
53 comparative reactivity method (CRM) (Sinha et al., 2008). A brief comparison of these  
54 techniques and known interferences has been summarized previously (Yang et al.,  
55 2016). In parallel with the developments of measuring techniques, total OH reactivity  
56 measurements have been intensively conducted in urban and suburban areas worldwide.  
57 Details of these campaigns are compared in Table 1 and Table 2, following similar  
58 summaries from previous papers (Lou et al., 2010; Dolgorouky et al., 2012; Yang et al.,  
59 2016). Most of the campaigns exhibited similar diel variations with higher reactivity in  
60 the late night and early morning rush hour, and lower results in the afternoon, which  
61 could be explained by the variations of the boundary layer height, the temporal change



62 in emissions and oxidation processes. Anthropogenic volatile organic compounds  
63 (VOCs) and inorganics, such as CO and NO<sub>x</sub> (NO + NO<sub>2</sub>) are major known OH sinks  
64 in urban areas.

65 However, a substantial difference between measured and calculated or modelled  
66 OH reactivity, which is termed missing reactivity, has been revealed in many campaigns.  
67 Compared to the high percentages of missing reactivity in forested areas (Sinha et al.,  
68 2010; Nölscher et al., 2012; 2016; Edwards et al., 2013, Williams et al., 2016), most  
69 campaigns reported relatively lower percentages of missing reactivity in urban and  
70 suburban areas except for the 75% missing reactivity in Paris in MEGAPOLI under  
71 continental air masses influences.

72 Different researchers have applied various methods in pursuit of origins of missing  
73 reactivity. Unmeasured primary species are important candidates. Sheehy et al. (2010)  
74 discovered a higher percentage of missing reactivity in morning rush hour and found  
75 unmeasured primary species, including organics with semi and low-volatility could  
76 contribute up to 10% reactivity. Direct measurements on reactivity of anthropogenic  
77 source emissions were conducted, such as vehicle exhaust and gasoline evaporation.  
78 An average of 17.5% missing reactivity was found in vehicle exhaust measurements  
79 (Nakashima et al., 2010), while good agreements were obtained for gasoline  
80 evaporation, by adding primary emitted branched-chained alkenes into consideration  
81 (Wu et al., 2015). All these experiments require more comprehensive measurements  
82 covering branched hydrocarbons as well as semi-volatile organic compounds (SVOCs).  
83 Besides primary substances, unknown secondary species are also not negligible.  
84 Yoshino et al. (2006) found a good correlation between missing reactivity and measured  
85 oxygenated VOCs (OVOCs) in three seasons except for winter, assuming that the  
86 unmeasured OVOCs could be major contributors of missing reactivity. The  
87 observation-based model (OBM) is widely used to evaluate the measured reactivity  
88 (Lee et al., 2010; Lou et al., 2010; Whalley et al., 2016), confirming the important  
89 contribution from OVOCs and undetected intermediate compounds, in one case could  
90 increase reactivity by over 50% (Lou et al., 2010).

91 Ground-level ozone has been of increasing concern in China. While the ozone



92 concentration exceeds Grade II of China National Ambient Air Quality Standards (2012)  
93 frequently in summer in Beijing-Tianjin-Hebei area and Pearl River Delta (PRD) region  
94 (Wang et al., 2006; Zhang et al., 2008), it appears there is an increasing trend for ozone  
95 in Beijing and other area (Zhao et al., 2009; Zhang et al., 2014). Due to the non-linearity  
96 relationship between the precursors ( $\text{NO}_x$  and VOCs) and ozone, revealing the  
97 contribution of VOCs to ozone formation has become a difficult but key question for  
98 researchers. Compared to traditional empirical kinetic model approach (EKMA)  
99 (Dodge et al., 1977), the OH reactivity due to VOCs (termed VOCs reactivity) rather  
100 than VOCs mixing ratio has certain advantages in the calculation of ozone production  
101 rate (Geddes et al., 2009; LaFranchi et al., 2011; Sinha et al., 2012; Zhang et al., 2014).  
102 However, due to species and chemistry deficiencies in measurements and model, the  
103 conception of VOCs reactivity was conventionally limited to the OH reactivity from  
104 measured species. Species, those have not yet been typically measured, hence  
105 unaccounted for, have laid a great uncertainty in ozone production prediction as well as  
106 in control strategy formulation. By directly measuring the total OH reactivity, VOCs  
107 reactivity can be obtained by deducting the inorganic reactivity from total OH reactivity,  
108 which provides a good constrain for the evaluation (Yang et al., 2016).

109 This paper presents two intensive observation datasets conducted in August 2013  
110 in Beijing, and October to November 2014 in Heshan, Guangdong, focusing on OH  
111 reactivity and related species. The variations of total OH reactivity at both sites were  
112 compared with similar observations in urban and suburban areas worldwide. Thereafter,  
113 a zero dimensional box model based on Regional Atmospheric Chemical Mechanism 2  
114 (RACM2) was employed for OH reactivity simulations. The possible missing reactivity  
115 was discussed and its importance for the ozone production calculation was also  
116 provided.

117

## 118 2. Methods

### 119 2.1 Total OH reactivity measurements

#### 120 2.1.1 Measuring principles

121 Total OH reactivity was measured by the comparative reactivity method first



122 developed at Max Planck Institute for Chemistry (Sinha et al., 2008). An introduction  
123 to the measurement system and principle is provided in brief below. The CRM system  
124 consisted of three major components, inlet and calibration system, reactor, and  
125 measuring system as in Fig 1. Ambient air was pumped through a 14.9m Teflon 3/8  
126 inch inlet at about 7 L·min<sup>-1</sup> rate.

127 In this method, pyrrole (C<sub>4</sub>H<sub>5</sub>N) was used as the reference substance and  
128 quantified by a quadrupole PTR-MS (Ionicon Analytic, Austria). There are four  
129 working modes for the whole measuring procedure. In the C0 mode, pyrrole (Air Liquid  
130 Ltd, U.S.) is introduced into the reactor with dry synthetic air (99.99%, Chengweixin  
131 Gas Ltd, China). A mercury lamp (185nm, used for OH radicals generation) is turned  
132 off and high-pure dry nitrogen (99.99%, Chengweixin Gas Ltd, China), is mixed into  
133 the reactor through a second arm. In this mode, the highest signals of m/z 68 (protonated  
134 mass of pyrrole) c0 are obtained. Then in the C1 mode, the nitrogen and synthetic air is  
135 still dry but the mercury lamp is turned on. The mixing ratio of pyrrole decreased to c1.  
136 The difference between c0 and c1 is mainly due to the photolysis of pyrrole (Sinha et  
137 al., 2008). C2 mode is the “zero air” mode in which synthetic air and nitrogen are  
138 humidified before being introduced into the reactor. The photolysis of water vapor  
139 generates OH radicals which react with pyrrole in the reactor to c2 level. Then C3 mode  
140 is the measuring mode in which the automatic valve switches from synthetic to ambient  
141 air. The ambient air is pumped into the reactor to react with OH radicals, competing  
142 with pyrrole molecules. The mixing ratio of pyrrole is detected as c3. Total OH  
143 reactivity is calculated as below, based on equations from Sinha et al. (2008):

$$144 \quad k_{OH} = c1 \times k_{Pyr+OH} \times \frac{c3-c2}{c1-c3} \quad (2-1)$$

### 145 **2.1.2 Calibrations and tests**

146 We performed two calibrations for the measurements. First, PTR-MS was  
147 calibrated by diluted dry pyrrole standard gas ranging from less than 10 ppbV to over  
148 160 ppbV (presented in Fig S1). Additionally, we conducted a comparison calibration  
149 with humidified pyrrole dilution gas. The sensitivity was about 3% to 5% higher than  
150 dry calibration, which was considered for later calculation (Sinha et al., 2009). The  
151 other calibration was to test the CRM system performance, in which single standard



152 gases, such as CO, propane, propene (Huayuan Gas Ltd, China) or a mixture 56 non-  
153 methane hydrocarbons (NMHCs) (SpecialGas Ltd, U.S.) were introduced into the CRM  
154 reactor instead of the ambient air samples. Examples of these calibrations are presented  
155 in Fig 2. Measured and calculated OH reactivity matched well within uncertainty range  
156 for all calibrations.

157 A major factor influencing the measurement results is the stability of OH radical  
158 generation. One potential interference is the difference in relative humidity between C2  
159 mode and C3 mode. During the experiment, we used one single needle valve to control  
160 the flow rate of synthetic air going through the bubbler, so that the relative humidity  
161 during C2 mode could be adjusted to match humidity during ambient sampling (C3  
162 mode). Meanwhile, the remaining minor difference could be corrected by factors  
163 derived from the OH reactivity-humidity correction experiment. The details of the OH-  
164 correction experiment and the figures are presented in the supporting information (Fig.  
165 S1 and S2).

166 Another interference is the variations of ambient NO, producing unconstrained  
167 OH radicals by recycling simultaneously generated HO<sub>2</sub> radicals, as described in  
168 previous studies (Sinha et al., 2008; Dolgorouky et al., 2012; Michoud et al., 2015). In  
169 the morning rush hour or on polluted cloudy days, NO can rise to over 30 ppbV in both  
170 Beijing and Heshan, which can potentially introduce high uncertainties for reactivity  
171 measurements. The NO-correction experiment was conducted by introducing known  
172 amounts of standard gases into the reactor. When the stable concentrations for c2 were  
173 obtained, different levels of NO were injected into the reactor and the “measured”  
174 reactivity decreased as the NO mixing ratio increased. Then a correction curve was  
175 fitted between the differences in reactivity and NO mixing ratios. Several standard  
176 gases and different levels of base reactivity (from less than 30s<sup>-1</sup> to over 180s<sup>-1</sup>) have  
177 been tried and the curve was quite consistent for all tested gases, as shown in Fig 3. The  
178 correction derived from the curve was used later to correct ambient measurements  
179 according to simultaneous detected NO levels. The correction was necessary when NO  
180 mixing ratio was larger than 5 ppbV, which was quite often observed in the morning  
181 time as well as cloudy days in Beijing and Heshan. The relative change for reactivity



182 results could be over  $100 \text{ s}^{-1}$  when NO mixing ratio was about 30 ppbV.

183 A further potential interference from nitrous acid (HONO) on total OH reactivity  
184 measurement with CRM was first discovered and corrected during the Heshan  
185 campaign. The photolysis of HONO in the reactor can generate the same amount of  
186 unconstrained OH radicals and NO molecules, as shown in R1. The additional OH  
187 radicals and NO molecules can be both interferences with the reactivity measurements.  
188 Similar correction experiments were conducted as the same with the NO correction  
189 experiment. HONO were added stepwise in several mixing ratios (1-10 ppbV),  
190 generated by a HONO generator (Liu et al., 2016) and thus introduced into the reactor.  
191 A curve was fitted between the differences in reactivity and HONO mixing ratios, as  
192 presented in Fig 4. The correction associated with this curve was also applied later in  
193 the ambient measurements.



195 To make sure the production of OH radicals was stable during the experiments, C1  
196 mode was measured for 1-2 hour every other day and C2 mode was measured for 20-  
197 30 minutes every two hours. With above calibrations and tests into consideration, the  
198 detection limits of CRM methods in two campaigns was around  $5 \text{ s}^{-1}$  ( $2\delta$ ). The total  
199 uncertainty of the method was about 20%, due to rate coefficient of pyrrole reactions  
200 (15%), flow fluctuation (3%), instrument precision (6% when measured reactivity  $> 15$   
201  $\text{ s}^{-1}$ ), standard gases (5%) and corrections for relative humidity (5%).

202

## 203 **2.2 Field measurements**

### 204 **2.2.1 Measuring sites and periods**

205 The urban measurements started from August 10<sup>th</sup> to August 27<sup>th</sup>, 2013 at Peking  
206 University (PKU) Site (116.18°E, 39.99°N), which was set on the roof laboratory of a  
207 6-floor building. The site is about 300 m from the 6 lane main road to the east and 500  
208 m off the 8 lane 4<sup>th</sup> ring of Beijing to the south. This site is a typical urban site and  
209 significantly impacted by vehicle emissions. Detailed information about this site can be  
210 found in a previous paper (Yuan et al., 2012).

211 Suburban measurements were conducted from October 20<sup>th</sup> to November 22<sup>nd</sup>



212 2014 at Heshan (HS) site, Guangdong (112.93°E, 22.73°N). The site is located on top  
213 of a small hill (60 m above ground) in Jiangmen, which is 50km from a medium size  
214 city Foshan (with a population of about 7 million) and 80 km from a megacity  
215 Guangzhou. Detailed information about this site can also be found in a separate paper  
216 (Fang et al., 2016)

### 217 **2.2.2 Simultaneous measurements**

218 During both intensive campaigns, fundamental meteorological parameters and  
219 trace gas were measured simultaneously. Meteorological parameters, such as  
220 temperature, relative humidity, pressure, wind speed, wind direction were measured.  
221 NO and NO<sub>x</sub> mixing ratios were measured by chemi-luminescence (model 42i, Thermo  
222 Fischer Inc, U.S.), and O<sub>3</sub> was measured by UV absorption (model 49i, Thermo Fischer  
223 Inc, U.S.). CO was measured by Gas Filter Correlation (model 48i, Thermo Fischer Inc,  
224 U.S.), and SO<sub>2</sub> was measured by pulsed fluorescence (model 43C, Thermo Fischer Inc,  
225 U.S.). The photolysis frequencies were measured by a spectral radiometer (SR)  
226 including 8 photolysis parameters. These parameters were all averaged into 1-minute  
227 resolution. The performances of these instruments are presented in Table S1 and Table  
228 S2.

229 VOCs were measured by a cryogen-free online GC-MSD/FID system, developed  
230 by Peking University (Yuan et al., 2012; Wang et al., 2014a). The time resolution is 1  
231 hour but the sampling time starts from the 5th minute to 10th minute every hour. The  
232 system was calibrated by two sets of standard gases: 56 NMHCs including 28 alkanes,  
233 13 alkenes and alkynes, 15 aromatics; EPA TO-15 standards  
234 (<http://www.epa.gov/ttnamti1/les/ambient/airtox/to-15r.pdf>), including additional  
235 OVOCs and halocarbons. The detection limits ranged from 10ppt-50ppt, depending on  
236 the species. Formaldehyde was measured by the Hantzsch method with time resolution  
237 of 1 minutes. Detailed information about this instrument is described in one previous  
238 paper (Li et al., 2014).

## 239 **2.3 Model description**

### 240 **2.3.1 Box model**

241 A zero-dimensional box model was applied to simulate the unmeasured secondary



242 products and OH reactivity for both field observations. The chemical mechanism  
 243 employed in the model was RACM2 (Stockwell et al., 1997, Goliff et al., 2013), with  
 244 implementation of the additional isoprene mechanism Mainz Isoprene Mechanism  
 245 (MIM, Pöschl et al., 2000) and update by Geiger et al. (2003) and Karl et al. (2006).  
 246 The model was constrained by measured photolysis frequencies, ancillary meteorology  
 247 and inorganic gases measurements, as well as VOCs results. Mixing ratios of methane  
 248 and H<sub>2</sub> were set to be 1.8 ppmV and 550 ppbV. The model was calculated in a time-  
 249 dependent mode with 5 min time resolution. In the model run, all input data were  
 250 constant in the time interval. Each model run started with 3 days spin-up time to reach  
 251 steady-state conditions for long-lived species. Additional loss by dry deposition was  
 252 assumed to have a corresponding lifetime of 24 hours to avoid the accumulation of  
 253 secondary productions.

### 254 2.3.2 Ozone production efficiency

255 Ozone production efficiency (OPE) is defined as the number of molecules of total  
 256 oxidants produced photochemically when a molecule of NO<sub>x</sub> was oxidized (Kleinman,  
 257 2002, Chou et al., 2011). It helps to evaluate the impacts of VOCs reactivity on ozone  
 258 production in various NO<sub>x</sub> regimes. In this model work, the OPE could be calculated  
 259 as the ratio of ozone production rate (i.e. P(O<sub>3</sub>)) to NO<sub>x</sub> consumption rate (i.e. D(NO<sub>x</sub>)).  
 260 NO<sub>z</sub>, calculated as the difference between NO<sub>y</sub> (sum of all odd-nitrogen compounds)  
 261 and NO<sub>x</sub>, was assumed to be the oxidation products of NO<sub>x</sub>. Thus the OPE could be  
 262 also calculated as P(O<sub>3</sub>)/P(NO<sub>z</sub>). The ozone production rate is obtained as 2-2, and the  
 263 P(NO<sub>z</sub>) is approximately as P(HNO<sub>3</sub>), which is given as 2-3.

$$264 \quad P(\text{O}_3) = k_{\text{HO}_2+\text{NO}} [\text{HO}_2][\text{NO}] + \sum_i k_{\text{RO}_2_i+\text{NO}} [\text{RO}_2_i][\text{NO}] \quad (2-2)$$

$$265 \quad P(\text{NO}_z) = k_{\text{NO}_2+\text{OH}} [\text{NO}_2][\text{OH}] \quad (2-3)$$

## 266 3. Results

### 267 3.1 Time series of meteorology and trace gases

268 In Fig 5, the time series of selected meteorological parameters and inorganic  
 269 trace gases are presented in 5 minute averages. The median values of the inorganic  
 270 trace gases were  $0.715 \pm 0.335$  ppmV for CO,  $6.3 \pm 5.75$  ppbV for NO and  $36.5 \pm$



271 21.3 ppbV for NO<sub>2</sub>, 57 ± 44 ppbV for O<sub>3</sub> in Beijing. In Heshan, the median results  
272 were 0.635 ± 0.355 for CO, 9.7 ± 6.95 for NO, 29.6 ± 12.6 for NO<sub>2</sub>, and 55.7 ± 34.9  
273 for O<sub>3</sub>. Both results were within the range of literature reports (Zhang et al., 2008;  
274 Zheng et al., 2010; Zhang et al., 2014). However, daytime averaged O<sub>3</sub> mixing ratio in  
275 Beijing 2013 was a little lower than the medium results (about 60 ppbV) in normal  
276 years (Zhang et al., 2014). This can be explained by higher frequencies of cloud and  
277 rains during the observations, taking up for one third of the measuring times. With  
278 weaker sunshine, the photolysis rate decreased significantly as the peak values of J  
279 (OID) on cloudy days could be only half the values of sunny days. Even with these  
280 factors into consideration, pollution episodes with ozone exceeding Grade II of China  
281 National Ambient Air Quality Standards (93 ppbV) existed in both campaigns.

282 Measured mixing ratios of VOCs in both campaigns are presented in Table S3  
283 and Table S4 in the supporting information. In summer Beijing, alkanes made up over  
284 60% of the summed VOCs during most of the time, while in Heshan the contribution  
285 from aromatics was 6% higher than that in Beijing. This could be explained by  
286 stronger emissions from solvent use and paint industry in the PRD region (Zheng et  
287 al., 2009). The ratio of toluene to benzene, which is typically used qualitatively as an  
288 indicator for aromatics emission sources also supported this assumption. While this  
289 ratio in Beijing was close to 2, similar to vehicle emissions (Barletta et al., 2005), the  
290 ratio in Heshan is higher than 3 due to strict control of benzene in solvent usage these  
291 days (Barletta et al., 2005; Liu et al., 2008). In the ozone polluted episode in Fig 5, the  
292 mixing ratios of most species were about twice to three times higher than the daily  
293 average results.

294 Comparing diurnal variations of NO<sub>x</sub>, O<sub>3</sub> and photochemical age, which are  
295 presented in Fig 6 and Fig 7, differences are apparent between both sites. Both sites  
296 presented similar diurnal patterns for O<sub>3</sub> and NO. However, the highest 1-hour  
297 average O<sub>3</sub> value at PKU site came in the afternoon and stayed in the high level till  
298 the dawn. However, O<sub>3</sub> pattern at Heshan site did not have the same “plateau” in the  
299 afternoon. An additional similarity was that NO peaks were present at similar times  
300 for both sites. But NO decreased at a slower rate in Heshan that even when it was



301 12:00 p.m., there was still over 1 ppbV. This was because NO observed at PKU site  
302 was mainly from local vehicle emissions while NO<sub>x</sub> at Heshan site was significantly  
303 influenced by transported air masses.

304 VOCs measurements provided us a good comparison of the oxidation state at  
305 two sites. Based on the OH exposure calculation methods (de Gouw et al., 2005), we  
306 chose a pair of VOCs species: m,p-xylene and ethylbenzene to calculate the  
307 photochemical age, as shown in 3-1

$$308 \quad [\text{OH}]\Delta t = [\ln(\frac{[E]}{[X]})_t - \ln(\frac{[E]}{[X]})_0] / (k_E - k_X) \quad (3-1)$$

309 Here, [E] and [X] represents the mixing ratios of ethylbenzene and m,p-xylene,  
310  $k_E$  and  $k_X$  means the OH reaction rate coefficient of ethylbenzene and m,p-xylene. As  
311 presented in Fig 7, we chose 1.15 ppbV ppbV<sup>-1</sup> and 2.3 ppbV ppbV<sup>-1</sup> as emission  
312 ratios of ethylbenzene to m,p-xylene in Beijing and Heshan, as they were the largest  
313 ratios in diurnal variations for the campaign. The largest OH exposure in Beijing 2013  
314 was calculated as  $0.71 \times 10^{11}$  mole s cm<sup>-3</sup> in 13:00 LTC, while the largest OH  
315 exposure in Heshan 2014 was calculated to be  $1.69 \times 10^{11}$  mole s cm<sup>-3</sup> in 14:00 LTC.  
316 The results in Beijing was comparable to previous reports (Yuan et al., 2012). Under  
317 the assumption that ambient OH concentration was  $8.0 \times 10^6$  mole cm<sup>-3</sup> (Lu et al.,  
318 2013), the photochemical age in Beijing was about 3 h at most. With measured peak  
319 OH concentration as  $1.2 \times 10^7$  mole cm<sup>-3</sup> in Heshan (Tan et al., in preparation), the  
320 photochemical age in Heshan was about 5 h to 6 h, which was about twice the  
321 photochemical age of the Beijing observations, indicating a more aged atmospheric  
322 environment in Heshan.

### 323 **3.2 Measured reactivity**

324 Total OH reactivity ranged from less than 10 s<sup>-1</sup> to over 100 s<sup>-1</sup> in Beijing  
325 summer 2013 (Fig 5a). The daily median value was  $19.98 \pm 11.03$  s<sup>-1</sup>, and presented a  
326 slight diel variation, despite the large variations between different days (Fig 8). Total  
327 OH reactivity was higher in the late night to morning rush hour with an hourly median  
328 value of 27.15 s<sup>-1</sup>, and decreased to a lower value in the afternoon, median value of  
329 17.33 s<sup>-1</sup>. This diurnal pattern was similar to the variations of NO<sub>x</sub> mixing ratios,



330 which was also presented in a previous study (Williams et al., 2016). The morning  
331 rush hour peak was mostly due to the stronger vehicle emissions from close roads.  
332 The difference between midnight reactivity and afternoon levels is the results of the  
333 variations of boundary layer height, vertical mixing and chemical reaction rates.

334 In contrast, measured total OH reactivity in Heshan was higher in median but the  
335 diel variation was not significant. The daily median value was  $30.62 \pm 19.76 \text{ s}^{-1}$ . The  
336 OH reactivity was much less variable in the daily variation. This could result from  
337 several “clean” periods with little variations for the whole day, during which ozone  
338 and  $\text{PM}_{2.5}$  concentrations were relatively low. Two pollution episodes were identified  
339 between October 24<sup>th</sup> to 27<sup>th</sup> and November 14<sup>th</sup> to 17<sup>th</sup>, 2014. Both episodes showed  
340 accumulating pollution with increasing concentrations of ozone and  $\text{PM}_{2.5}$ . The  
341 reactivity level was also significantly higher than ordinary days (Fig 5b).

### 342 3.3 Variations in missing reactivity

343 Significant differences between measured and calculated reactivity have been  
344 obtained for both measurements in Beijing and Heshan. While the measured reactivity  
345 was obtained by direct measurement, the calculated reactivity was derived from mixing  
346 ratios of different species multiplied by their rate coefficients with OH radicals. Taking  
347 all measured species into consideration,  $\text{NO}_x$  and NMHCs contributed the most, which  
348 were 45%-55% of total OH reactivity (Fig 9). However, measured OVOCs played a  
349 more significant role in Beijing rather than in Heshan, due to higher levels of  
350 formaldehyde and acetaldehyde observed in Beijing. This could be partially explained  
351 by the seasonal difference and thus faster photochemical productions in August in  
352 Beijing than October and November in Heshan.

353 Missing reactivity was on average  $21 \pm 17\%$  of the total OH reactivity in Beijing  
354 and  $32 \pm 21\%$  in Heshan. However, the missing reactivity presented different temporal  
355 patterns. In Beijing, the missing reactivity was extremely high during pollution  
356 episodes. On some occasions during the morning rush hour, the missing percentage  
357 reached over 50%. In contrast, missing reactivity was quite consistent for the whole  
358 campaign at the Heshan site, similar to measured reactivity patterns. Even for clean  
359 days with reactivity levels of less than  $20 \text{ s}^{-1}$ , a 20%-30% percentage of missing



360 reactivity still existed.

## 361 **4. Discussion**

### 362 **4.1 Reactivity levels in Beijing and Heshan**

363 While the absolute VOCs reactivity was high for both sites, the relative reactivity  
364 compared to NMHCs mixing ratios were higher. Compared to other urban and suburban  
365 measurements, the measured VOCs reactivity (obtained by subtracting inorganic  
366 reactivity from total OH reactivity) was not very high (Beijing 2013 as  $11.2\text{s}^{-1}$  and  
367 Heshan 2014 as  $18.3\text{s}^{-1}$ ), as in Fig 10. Tokyo presented a similar level of VOCs  
368 reactivity (Yoshino et al., 2006) and Paris had an even higher level of VOCs reactivity  
369 despite the observation was conducted in the winter (Dolgorouky et al., 2012). The  
370 measured NMHCs levels (obtained by adding all hydrocarbon mixing ratios together)  
371 were also not very high, with Beijing 2013 being around 20 ppbV and Heshan 2014  
372 higher than 35 ppbV. However, when the VOCs reactivity was divided by the measured  
373 NMHCs mixing ratios to obtain the ratio, values for both Beijing and Heshan were  
374 higher than results from similar observations. This indicated that with a similar level of  
375 hydrocarbons, VOCs in Beijing and Heshan would provide higher reactivity than in  
376 other areas.

377 There could be several explanations for this phenomenon. One possible  
378 explanation is the higher contribution from highly-reactive VOCs. Compared to other  
379 campaigns, both observation sites in this study had a slightly higher loading of alkenes  
380 and aromatics (Yuan et al., 2012; Wang et al., 2014b). These species significantly  
381 increased the VOCs reactivity due to relatively higher OH reaction rate coefficients.  
382 The other probable reason is contribution from OVOCs. In Beijing and PRD,  
383 formaldehyde could accumulate to over 10 ppbV during some periods, which was  
384 significantly higher than levels found in other observations (Li et al., 2013; Chen et al.,  
385 2014). Another possible explanation is unmeasured species, whether primary  
386 hydrocarbons or secondary products, which will be discussed later.

### 387 **4.2 Contributions to the missing reactivity: primary VOCs**

388 As missing reactivity was observed at Beijing and Heshan site during both



389 campaigns, the species causing these missing phenomena were examined. One possible  
390 explanation could be unmeasured primary VOCs species.

391 Throughout the whole campaign at the PKU site, missing reactivity was normally  
392 found in the morning, as for an example in August 16<sup>th</sup> and 17<sup>th</sup> 2013 in Fig 11. Between  
393 5 a.m. to 10 a.m., primary emissions were strong due to vehicle-related sources, but the  
394 chemical reactions were relatively slow owing to comparatively weak sunshine, and  
395 thus low concentrations of oxidants. Unmeasured primary VOCs species were therefore  
396 assumed to be the most likely contributors to missing reactivity in this time range.  
397 Specially unmeasured branched-alkenes were paid attention to, for their high reactivity  
398 and previously observed emissions from vehicle exhaust (Nakashima et al., 2010) and  
399 gasoline evaporation (Wu et al., 2015). We found only one dataset in 2005 measured  
400 by NOAA (Liu et al., 2009). We chose the diurnal patterns of missing reactivity in  
401 Beijing 2013 and compared to the diel cycles of four measured branched-alkenes in  
402 2005. Good correlations were found as presented in Fig 11. However, even with mixing  
403 ratios of 2005, the reactivity contribution was less than  $2.5\text{s}^{-1}$ . With observed decreasing  
404 trends in mixing ratios of most NMHCs species in Beijing (Zhang et al., 2014; Wang et  
405 al., 2015), the branched-alkenes were insufficient to explain the missing reactivity.  
406 Unmeasured semi-volatile organic compounds (SVOCs) and intermediate volatile  
407 organic compounds (IVOCs), such as alkanes between C<sub>12</sub> to C<sub>30</sub>, and polycyclic  
408 aromatic hydrocarbons (PAHs) could be also important. Sheehy (2010) found SVOCs  
409 and IVOCs contributed to about 10% in morning time in Mexico City. A more  
410 comprehensive characterization of VOCs covering high-volatility to low-volatility is  
411 required for future budget closure experiments of total OH reactivity.

#### 412 **4.3 Contributions to the missing reactivity: secondary VOCs**

413 Due to limitations in chemistry mechanisms as well as measuring techniques,  
414 secondary products are not fully quantified in ambient air and could probably contribute  
415 significantly to the observed missing reactivity, especially in the urban or suburban sites  
416 receiving chemically complex aged air masses.

417 Besides the large missing reactivity during the morning rush hour, there was about  
418 25% difference between measured and calculated reactivity from August 16<sup>th</sup> to 18<sup>th</sup>,



419 2013 at PKU site. Considering high levels of oxidants in daytime, the mixing ratios of  
420 branched-alkenes could be lower than 0.1 ppbV, which could not explain the observed  
421 missing reactivity. Constrained by measured parameters (meteorology, inorganic gases,  
422 VOCs including measured carbonyls), modeled reactivity was about 20-25% higher  
423 than calculated reactivity and could agree with measured reactivity in most of the  
424 daytime, as presented in Fig 11. Major contributors from modeled species were  
425 unmeasured aldehydes, glyoxal and methyl glyoxal. Average values of major secondary  
426 contributors to modelled reactivity are provided in Table S5. In the model, the higher  
427 secondary contribution on August 17<sup>th</sup> 2013 morning was owing to isoprene oxidation  
428 products due to unusual high levels of isoprene over 1.5 ppbV at 8:00 a.m. However,  
429 there remained over 40% missing reactivity at 7:00 and 8:00 a. m. unexplained within  
430 the model.

431 The similar OBM was applied for the Heshan observation to simulate the  
432 unmeasured secondary species, as shown in Fig 12. During the heavy polluted episode  
433 between October 24<sup>th</sup> and 27<sup>th</sup> 2014, a 30% missing reactivity existed for most time  
434 between the measured reactivity and the calculated reactivity. However, the modeled  
435 reactivity was only about 10-20% higher than calculated reactivity, and not enough to  
436 explain the measured reactivity. The major contributors among modeled species were  
437 also unmeasured aldehydes, glyoxal, methyl glyoxal and other secondary products, as  
438 shown in Table S6. Due to strong emissions of aromatics from solvent use and  
439 petroleum industry in PRD region (Zheng et al., 2009), high levels of glyoxal and  
440 methyl glyoxal in this region have been observed from space borne measurements (Liu  
441 et al., 2012) and ground-based measurements (Li et al., 2013). Compared to the 2006  
442 measurements in Backgarden, a semi-rural site in PRD region, the modeled glyoxal was  
443 twice as high as around 0.8 ppbV (Li et al., 2013). This difference possibly resulted  
444 from higher levels of precursors in 2014 measurements, where the measured reactivity  
445 was about 50% higher than the results in Backgarden 2006 (Lou et al., 2010).

#### 446 **4.4 Implications for ozone production efficiency**

447 While the missing reactivity raises our interests in looking for unknown organic  
448 species in measurements and simulations, it also provides a useful constrain for ozone



449 modelling, which lead us to wonder how much the unconstrained VOCs species will  
450 contribute to ozone production. To evaluate this contribution, we employed the OBM  
451 model to calculate the OPE. We set two scenarios for the model run: 1) The base run  
452 was constrained with measured species, including all inorganic compounds, PAMS 56  
453 hydrocarbons, TO-15 OVOCs and formaldehyde. This is how we obtained the modelled  
454 reactivity as presented above. With the model's help, some intermediates and oxidation  
455 products were reproduced. 2) The other scenario was constrained by measured  
456 reactivity. However, due to the difference between measured and modeled reactivity,  
457 we allocated the missing reactivity into several groups. For the primary species, we  
458 assumed the ratio between total chain-alkenes and branched-alkenes were the same in  
459 Beijing 2013 and in Heshan 2014 as the ratio in Beijing 2005, so we got the assumed  
460 mixing ratios of branched-alkenes at both sites. For secondary species, we allocated the  
461 remaining missing reactivity into different intermediates or products based on weights  
462 obtained in the model base run. Under both assumptions, we ran the OBM and  
463 calculated the OPE, as presented in Fig 13.

464 For both sites, the OPE constrained by measured reactivity were significantly  
465 higher than the OPE we calculated from modeled reactivity. In Beijing, the OPE from  
466 measured reactivity was about 27% higher in average. The value was 35% higher at  
467 Heshan site under similar assumptions. This percentage was close to the percentage of  
468 missing reactivity, indicating the ignorance of unmeasured or unknown organic species  
469 can cause significant underestimation in ozone production calculation.

470 Compared to other similar calculations worldwide, the OPE results for Beijing and  
471 Heshan were significantly higher (Fig 14). The comparison was made for  $\text{NO}_x = 20$   
472 ppbV which was in the range of most observation results. For urban measurements,  
473 only the results from Mexico City in MCMA-03 were close to the Beijing results in  
474 basic model run (Lei et al., 2008). For suburban measurements, the OPE in Heshan  
475 2014 was higher than all other three campaigns, even including the results from  
476 Shangdianzi station in CAREBEIJING-2008 campaigns (Ge et al., 2012). While taking  
477 missing reactivity into consideration, the OPE results were even higher, indicating more  
478 ozone was produced by the reactions of the same quantity of  $\text{NO}_x$  molecules.



## 479 5. Conclusions

480 In this study, total OH reactivity measurements employing CRM system were  
481 conducted at PKU site in Beijing 2013, and Heshan site 2014 in PRD region.  
482 Comparisons between measured and calculated, as well as modelled reactivity were  
483 made and possible reasons for the missing reactivity have been investigated. The  
484 contribution of missing reactivity to ozone production efficiency was evaluated.

485 In Beijing 2013, daily median result for measured total OH reactivity was  $19.98 \pm$   
486  $11.03 \text{ s}^{-1}$ . Similar diurnal variation with other urban measurements was found with  
487 peaks over  $25 \text{ s}^{-1}$  during the morning rush hour and lower reactivity than  $16 \text{ s}^{-1}$  in the  
488 afternoon. In Heshan 2014, total OH reactivity was  $30.62 \pm 19.76 \text{ s}^{-1}$  on daily median  
489 result. The diurnal variation was not significant. Both sites have experienced OH  
490 reactivity over  $80 \text{ s}^{-1}$  during polluted episodes.

491 Missing reactivity was found at both sites. While in Beijing the missing reactivity  
492 made up 21% of measured reactivity, some periods even reached a higher missing  
493 percentage as 40%-50%. In Heshan, missing reactivity's contribution to total OH  
494 reactivity was 32% on average and quite stable for the whole day. Unmeasured primary  
495 species, such as branched-alkenes could be important contributor to the missing  
496 reactivity in Beijing, especially in morning rush hour, but they were not enough to  
497 explain Aug 17<sup>th</sup> morning's event. With the help of RACM2, unmeasured secondary  
498 products were calculated and thus the modelled reactivity could agree with measured  
499 reactivity in Beijing in the noontime. However, they were still not enough to explain  
500 the missing reactivity in Heshan, even in daytime. This was probably because of the  
501 relatively higher oxidation stage in Heshan than in Beijing.

502 Missing reactivity could impact the estimation of atmospheric ozone production  
503 efficiency. Compared to modeled reactivity from base run, ozone production efficiency  
504 would rise 27% and 35% in Beijing and Heshan with measured reactivity applied. Both  
505 results were significantly higher than similar observations worldwide, indicating the  
506 relatively faster ozone production at both sites.

507 However, in order to further explore the OH reactivity in both regions, more



508 species need to be included in measurements and modeling to close the total OH  
509 reactivity budget. Moreover, a thorough way with more detailed mechanisms should be  
510 established to connect the missing reactivity to the evaluation of ozone production.

511

### 512 **Acknowledgement**

513 This study was funded by the Natural Science Foundation for Outstanding Young  
514 Scholars (grant no. 41125018) and a Natural Science Foundation key project (grant  
515 no.411330635). The research was also supported by the European Commission  
516 Partnership with China on Space Data (PANDA project). Special thanks to Jing Zheng,  
517 Mei Li, Yuhan Liu from Peking University and Tao Zhang from Guangdong  
518 Environmental Monitoring Center for the help, thanks for William. C. Kuster from  
519 NOAA . Earth System Research Laboratory for the branched-alkenes data in 2005.

520

521

522

523

524

525

526

527

528

529

530

531

532

533

534

535

### 536 **Reference**



- 537 Barletta, B., Meinardi, S., Sherwood Rowland, F., Chan, C.-Y., Wang, X., Zou, S., Yin  
538 Chan, L., and Blake, D. R.: Volatile organic compounds in 43 Chinese cities, Atmos.  
539 Environ., 39, 5979-5990, doi: 10.1016/j.atmosenv.2005.06.029, 2005.
- 540 Calpini, B., Jeanneret, F., Bourqui, M., Clappier, A., Vajtai, R., and van den Bergh, H.:  
541 Direct measurement of the total reaction rate of OH in the atmosphere, *Analisis*, 27,  
542 328-336, doi: 10.1051/analisis:1999270328, 1999.
- 543 Chatani, S., Shimo, N., Matsunaga, S., Kajii, Y., Kato, S., Nakashima, Y., Miyazaki, K.,  
544 Ishii, K., and H., U.: Sensitivity analyses of OH missing sinks over Tokyo metropolitan  
545 area in the summer of 2007, *Atmos. Chem. Phys.*, 9, 8975-8986, doi: 10.5194/acp-9-  
546 8975-2009, 2009.
- 547 Chen, W. T., Shao, M., Lu, S. H., Wang, M., Zeng, L. M., Yuan, B., Liu, Y.:  
548 Understanding primary and secondary sources of ambient carbonyl compounds in  
549 Beijing using the PMF model. *Atmos. Chem. Phys.*, 14, 3047-3062, doi: 10.5194/acp-  
550 14-3047-2014, 2014.
- 551 Chou, C. C. K., Tsai, C. Y., Chang, C. C., Lin, P. H., Liu, S. C., and Zhu, T.:  
552 Photochemical production of ozone in Beijing during the 2008 Olympic Games, *Atmos.*  
553 *Chem. Phys.*, 11, 9825-9837, doi: 10.5194/acp-11-9825-2011, 2011.
- 554 Dodge, M. C.: Proceedings of the international conference on photochemical oxidant  
555 pollution and its control. Combined use of modeling techniques and smog chamber data  
556 to derive ozone-precursor relationships, U.S. Environmental Protection Agency,  
557 Research Triangle Park, NC, 881-889 pp., 1977.
- 558 de Gouw, J. A., Middlebrook, A. M., Warneke, C., Goldan, P. D., Kuster, W. C., Roberts,  
559 J. M., Fehsenfeld, F. C., Worsnop, D. R., Canagaratna, M. R., Pszenny, A. A. P., Keene,  
560 W. C., Marchewka, M., Bertman, S. B., Bates, T. S.: Budget of organic carbon in a  
561 polluted atmosphere: Results from the New England Air Quality Study in 2002, *J.*  
562 *Geophys. Res.-Atmos.*, 110, D16305, doi: 10.1029/2004jd005623, 2005.
- 563 Dolgorouky, C., Gros, V., Sarda-Esteve, R., Sinha, V., Williams, J., Marchand, N.,  
564 Sauvage, S., Poulain, L., Sciare, J., and Bonsang, B.: Total OH reactivity measurements  
565 in Paris during the 2010 MEGAPOLI winter campaign, *Atmos. Chem. Phys.*, 12, 9593-  
566 9612, doi: 10.5194/acp-12-9593-2012, 2012.
- 567 Edwards, P. M., Evans, M. J., Furneaux, K. L., Hopkins, J., Ingham, T., Jones, C., Lee,  
568 J. D., Lewis, A. C., Moller, S. J., Stone, D., Whalley, L. K., and Heard, D. E.: OH  
569 reactivity in a South East Asian tropical rainforest during the Oxidant and Particle  
570 Photochemical Processes (OP3) project, *Atmos. Chem. Phys.*, 13, 9497-9514, doi:



- 571 10.5194/acp-13-9497-2013, 2013.
- 572 Fang, X., Shao, M., Stohl, A., Zhang, Q., Zheng, J., Guo, H., Wang, C., Wang, M., Ou,  
573 J., Thompson, R. L., and Prinn, R. G.: Top-down estimates of benzene and toluene  
574 emissions in the Pearl River Delta and Hong Kong, China, *Atmos. Chem. Phys.*, 16,  
575 3369-3382, doi: 10.5194/acp-16-3369-2016, 2016.
- 576 Fuchs, H., Hofzumahaus, A., Rohrer, F., Bohn, B., Brauers, T., Dorn, H. P., Häseler, R.,  
577 Holland, F., Kaminski, M., Li, X., Lu, K., Nehr, S., Tillmann, R., Wegener, R., and  
578 Wahner, A.: Experimental evidence for efficient hydroxyl radical regeneration in  
579 isoprene oxidation, *Nature Geoscience*, 6, 1023-1026, doi: 10.1038/ngeo1964, 2013.
- 580 Ge. B. Z., Sun. Y. L., Liu. Y., Dong. H. B., Ji. D. S., Jiang. Q., Li. J., Wang. Z. F.:  
581 Nitrogen dioxide measurement by cavity attenuated phase shift spectroscopy (CAPS)  
582 and implications in ozone production efficiency and nitrate formation in Beijing, China.  
583 *J. Geophys. Res.-Atmos.*, 118, 9499-9509, doi: 10.1002/jgrd.50757, 2013.
- 584 Geddes, J. A., Murphy, J. G., and K., W. D.: Long term changes in nitrogen oxides and  
585 volatile organic compounds in Toronto and the challenges facing local ozone control,  
586 *Atmos. Environ.*, 43, 3407-3415, doi: 10.1016/j.atmosenv.2009.03.053, 2009.
- 587 Geiger, H., Barnes, I., Bejan, I., Benter, T., and Spittler, M.: The tropospheric  
588 degradation of isoprene: an updated module for the regional atmospheric chemistry  
589 mechanism, *Atmos. Environ.*, 37, 1503-1519, doi: 10.1016/S1352-2310(02)01047-6,  
590 2003.
- 591 Goliff, W. S., Stockwell, W. R., Lawson, C. V.: The regional atmospheric chemistry  
592 mechanism, version 2. *Atmos. Environ.*, 68, 174-185, doi: 10.1016/j.atmosenv.2012.11.  
593 038, 2013
- 594 Hansen, R. F., Blocquet, M., Schoemaeker, C., Léonardis, T., Locoge, N., Fittschen,  
595 C., Hanoune, B., Stevens, P. S., Sinha, V., and Dusanter, S.: Intercomparison of the  
596 comparative reactivity method (CRM) and pump-probe technique for measuring total  
597 OH reactivity in an urban environment, *Atmos. Meas. Tech.*, 8, 4243-4264, doi:  
598 10.5194/amt-8-4243-2015, 2015.
- 599 Ingham, T., Goddard, A., Whalley, L. K., Furneaux, K. L., Edwards, P. M., Seals, C. P.,  
600 Self, D. E., Johnson, G. P., Read, K. A., Lee, J. D., and E., H. D.: a flow tube based LIF  
601 instrument to measure OH reactivity in the troposphere, *Atmos. Meas. Tech.*, 2, 465-  
602 477, doi: 10.5194/amt-2-465-2009, 2009.
- 603 Karl, M., Dorn, H.-P., Holland, F., Koppmann, R., Poppe, D., Rupp, L., Schaub, A., and  
604 Wahner, A.: Product study of the reaction of OH radicals with isoprene in the



- 605 atmosphere simulation chamber SAPHIR, *J. Atmos. Chem.*, **55**, 167–187, doi:  
606 10.1007/s10874-006-9034-x, 2006.
- 607 Kato, S., Sato, T., Kaji, Y.: A method to estimate the contribution of unidentified VOCs  
608 to OH reactivity. *Atmos. Environ.*, **45**, 5531-5539, doi: 10.1016/j.atmosenv.2011.05.  
609 074. 2011.
- 610 Kleinman, L. I., Daum, P. H., Imre, D. G., Lee, J. H., Lee, Y. N., Nunnermacker, L. J.,  
611 Springston, S. R., Weinstein-Lloyd, J., Newman, L.: Ozone production in the New York  
612 City urban plume. *J. Geophys. Res.-Atmos.*, **105**, D11, 14495-14511, doi: 10.1029/2000  
613 jd900011, 2000.
- 614 Kleinman, L. I.: Ozone production efficiency in an urban area, *J. Geophys. Res. – atmos.*,  
615 **107**, D23, 4733, doi: 10.1029/2002jd002529, 2002.
- 616 Kovacs, T. A., and Brune, W. H.: Total OH loss rate measurement, *J. Atmos. Chem.*,  
617 **39**, 105-122, doi: 10.1023/a:1010614113786, 2001.
- 618 Kovacs, T. A., Brune, W. H., Harder, H., Martinez, M., Simpas, J. B., Frost, G. J.,  
619 Williams, A. G., Jobson, B. T., Stroud, C., Young, V., Fried, A., and B., W.: Direct  
620 measurements of urban OH reactivity during Nashville SOS in summer 1999, *J.*  
621 *Environ. Monit.*, **5**, 68-74, doi: 10.1039/b204339d, 2003.
- 622 LaFranchi, B. W., Goldstein, A. H., and Cohen, R. C.: Observations of the temperature  
623 dependent response of ozone to NO<sub>x</sub> reductions in the Sacramento, CA urban plume,  
624 *Atmos. Chem. Phys.*, **11**, 6945-6960, doi: 10.5194/acp-11-6945-2011, 2011.
- 625 Lee, J. D., Young, J. C., Read, K. A., Hamilton, J. F., Hopkins, J. R., Lewis, A. C.,  
626 Bandy, B. J., Davey, J., Edwards, P. M., Ingham, T., Self, D. E., Smith, S. C., Pilling,  
627 M. J., and Heard, D. E.: Measurement and calculation of OH reactivity at a United  
628 Kingdom coastal site, *J. Atmos. Chem.*, **64**, 53-76, doi: 10.1007/s10874-010-9171-0,  
629 2010.
- 630 Lei, W., Zavala, M., Foy, B. de., Volkamer, R., Molina, L. T.: Characterizing ozone  
631 production and response under different meteorological conditions in Mexico City.  
632 *Atmos. Chem. Phys.*, **8**, 7571-7581, doi: 10.5194/acp-8-7571-2008, 2008.
- 633 Li, M., Shao, M., Li, L.-Y., Lu, S.-H., Chen, W.-T., and Wang, C.: Quantifying the  
634 ambient formaldehyde sources utilizing tracers, *Chinese. Chem. Lett.*, **25**, 1489-1491,  
635 doi: 10.1016/j.ccllet.2014.07.001, 2014.
- 636 Li, X., Brauers, T., Hofzumahaus, A., Lu, K., Li, Y. P., Shao, M., Wagner, T., and  
637 Wahner, A.: MAX-DOAS measurements of NO<sub>2</sub>, HCHO and CHOCHO at a rural site  
638 in Southern China, *Atmos. Chem. Phys.*, **13**, 2133-2151, doi: 10.5194/acp-13-2133-



- 639 2013, 2013.
- 640 Liu, Y., Shao, M., Fu, L., Lu, S., Zeng, L., and Tang, D.: Source profiles of volatile  
641 organic compounds (VOCs) measured in China: Part I, Atmos. Environ., 42, 6247-6260,  
642 doi: 10.1016/j.atmosenv.2008.01.070, 2008.
- 643 Liu, Y., Shao, M., Kuster, W. C., Goldan, P. D., Li, X. H., Lu, S. H., de Gouw, J. A.:  
644 Source identification of reactive hydrocarbons and oxygenated VOCs in the  
645 summertime in Beijing. Environ. Sci. Technol., 43, 75-81, doi: 10.1021/es801716n,  
646 2009.
- 647 Liu, Y. H., Lu, K. D., Dong, H. B., Li, X., Cheng, P., Zou, Q., Wu, Y. S., Liu, X. G.,  
648 Zhang, Y. H. In situ monitoring of atmospheric nitrous acid based on multi-pumping  
649 flow system and liquid waveguide capillary cell. J. Environ. Sci. Accepted. 2016.
- 650 Liu, Z., Wang, Y., Vrekoussis, M., Richter, A., Wittrock, F., Burrows, J. P., Shao, M.,  
651 Chang, C.-C., Liu, S.-C., Wang, H., and Chen, C.: Exploring the missing source of  
652 glyoxal (CHOCHO) over China, Geophys. Res. Lett., 39, L10812, doi:  
653 10.1029/2012gl051645, 2012.
- 654 Lou, S., Holland, F., Rohrer, F., Lu, K., Bohn, B., Brauers, T., Chang, C. C., Fuchs, H.,  
655 Häsel, R., Kita, K., Kondo, Y., Li, X., Shao, M., Zeng, L., Wahner, A., Zhang, Y.,  
656 Wang, W., and Hofzumahaus, A.: Atmospheric OH reactivities in the Pearl River Delta  
657 – China in summer 2006: measurement and model results, Atmos. Chem. Phys., 10,  
658 11243-11260, doi: 10.5194/acp-10-11243-2010, 2010.
- 659 Lu, K. D., Zhang, Y. H., Su, H., Brauers, T., Chou, C. C., Hofzumahaus, A., Liu, S. C.,  
660 Kita, K., Kondo, Y., Shao, M., Wahner, A., Wang, J. L., Wang, X., and T., Z.: Oxidant  
661 ( $O_3 + NO_2$ ) production processes and formation regimes in Beijing, J. Geophys. Res.-  
662 Atmos., 115, D07303, doi: 10.1029/2009jd012714, 2010.
- 663 Lu, K. D., Hofzumahaus, A., Holland, F., Bohn, B., Brauers, T., Fuchs, H., Hu, M.,  
664 Häsel, R., Kita, K., Kondo, Y., Li, X., Lou, S. R., Oebel, A., Shao, M., Zeng, L. M.,  
665 Wahner, A., Zhu, T., Zhang, Y. H., and Rohrer, F.: Missing OH source in a suburban  
666 environment near Beijing: observed and modelled OH and HO<sub>2</sub> concentrations in  
667 summer 2006, Atmos. Chem. Phys., 13, 1057-1080, doi: 10.5194/acp-13-1057-2013,  
668 2013.
- 669 Mao, J. Q., Ren, X. R., Chen, S., Brune, W. H., Chen, Z., Martinez, M., Harder, H.,  
670 Lefer, B., Rappengluck, B., Flynn, J., and M., L.: Atmospheric oxidation capacity in  
671 the summer of Houston 2006: Comparison with summer measurements in other  
672 metropolitan studies, Atmos. Environ., 44, 4107-4115, doi: 10.1016/j.atmosenv.2009.



- 673 01.013, 2010.
- 674 Michoud, V., Hansen, R. F., Locoge, N., Stevens, P. S., and Dusanter, S.: Detailed  
675 characterizations of the new Mines Douai comparative reactivity method instrument  
676 via laboratory experiments and modeling, *Atmos. Meas. Tech.*, 8, 3537-3553, doi:  
677 10.5194/amt-8-3537-2015, 2015.
- 678 Nölscher, A. C., Williams, J., Sinha, V., Custer, T., Song, W., Johnson, A. M., Axinte,  
679 R., Bozem, H., Fischer, H., Pouvesle, N., Phillips, G., Crowley, J. N., Rantala, P., Rinne,  
680 J., Kulmala, M., Gonzales, D., Valverde-Canossa, J., Vogel, A., Hoffmann, T.,  
681 Ouwersloot, H. G., Vilà-Guerau de Arellano, J., and Lelieveld, J.: Summertime total  
682 OH reactivity measurements from boreal forest during HUMPPA-COPEC 2010, *Atmos.*  
683 *Chem. Phys.*, 12, 8257-8270, doi: 10.5194/acp-12-8257-2012, 2012.
- 684 Nölscher, A. C., Yanez-Serrano, A. M., Wolff, S., de Araujo, A. C., Lavric, J. V.,  
685 Kesselmeier, J., and Williams, J.: Unexpected seasonality in quantity and composition  
686 of Amazon rainforest air reactivity, *Nature communications*, 7, 10383-10394, doi:  
687 10.1038/ncomms10383, 2016.
- 688 Nakashima, Y., Kamei, N., Kobayashi, S., and Y., K.: Total OH reactivity and VOC  
689 analyses for gasoline vehicular exhaust with a chassis dynamometer, *Atmos. Environ.*,  
690 44, 468-475, doi: 10.1016/j.atmosenv.2009.11.006, 2010.
- 691 Pöschl, U., von Kuhlmann, R., Poisson, N., and Crutzen, P. J.: Development and  
692 intercomparison of condensed isoprene oxidation mechanisms for global atmospheric  
693 modeling, *J. Atmos. Chem.*, 37, 29-52, doi: 10.1023/A:1006391009798, 2000.
- 694 Ren, X. R., Harder, H., Martinez, M., Leshner, R. L., Olinger, A., Shirley, T., Adams, J.,  
695 Simpas, J. B., and H., B. W.: HO<sub>x</sub> concentrations and OH reactivity observations in  
696 New York City during PMTACS-NY2001, *Atmos. Environ.*, 37, 3627-3637, doi:  
697 10.1016/s1352-2310(03)00460-6, 2003.
- 698 Ren, X. R., Brune, W. H., Cantrell, C., Edwards, G. D., Shirley, T., Metcalf, A. R., and  
699 L., L. R.: Hydroxyl and Peroxy Radical Chemistry in a Rural Area of Central  
700 Pennsylvania: Observations and Model Comparisons, *J. Atmos. Chem.*, 52, 231-257,  
701 doi: 10.1007/s10874-005-3651-7, 2005.
- 702 Ren, X. R., Brune, W. H., Mao, J. Q., Mitchell, M. J., Leshner, R. L., Simpas, J. B.,  
703 Metcalf, A. R., Schwab, J. J., Cai, C., and Y., L.: Behavior of OH and HO<sub>2</sub> in the winter  
704 atmosphere in New York City, *Atmos. Environ.* 40, 252-263, doi: 10.1016/j.atmosenv.  
705 2005.11.073, 2006a.
- 706 Ren, X. R., Brune, W. H., Olinger, A., Metcalf, A. R., Simpas, J. B., Shirley, T., Schwab,



- 707 J. J., Bai, C., Roychowdhury, U., Li, Y., Cai, C., Demerjian, K. L., He, Y., Zhou, X. H.,  
708 Gao, H., and J., H.: OH, HO<sub>2</sub>, and OH reactivity during the PMTACS–NY Whiteface  
709 Mountain 2002 campaign: Observations and model comparison, *J. Geophys. Res.-*  
710 *Atmos.*, 111, doi: 10.1029/2005jd006126, 2006b.
- 711 Sadanaga, Y., Yoshino, A., Kato, S., Yoshioka, A., Watanabe, K., Miyakawa, T.,  
712 Hayashi, I., Ichikawa, M., Matsumoto, J., Nishiyama, A., Akiyama, N., Kanaya, Y., and  
713 Y., K.: The importance of NO<sub>2</sub> and volatile organic compounds in the urban air from  
714 the viewpoint of the OH reactivity, *Geophys. Res. Lett.*, 31, L08102, doi:  
715 10.1029/2004gl019661, 2004.
- 716 Sadanaga, Y., Yoshino, A., Kato, S., and Y., K.: measurements of OH reactivity and  
717 photochemical ozone production in the urban atmosphere, *Environ. Sci. Technol.*, 39,  
718 8847-8852, doi: 10.1021/es049457p, 2005.
- 719 Sheehy, P. M., Volkamer, R., Molina, L. T., and Molina, M. J.: Oxidative capacity of  
720 the Mexico City atmosphere – Part 2: A RO<sub>x</sub> radical cycling perspective, *Atmos. Chem.*  
721 *Phys.*, 10, 6993-7008, doi: 10.5194/acp-10-6993-2010, 2010.
- 722 Shirley, T. R., Brune, W. H., Ren, X. R., Mao, J. Q., Leshner, R., Cardenas, B., Volkamer,  
723 R., Molina, L. T., Molina, M. J., Lamb, B., Velasco, E., Jobson, T., and M., A.:  
724 Atmospheric oxidation in the MCMA during April 2003, *Atmos. Chem. Phys.*, 6, 2753-  
725 2765, doi: 10.5194/acp-6-2753-2006, 2006.
- 726 Sinha, V., Williams, J., Crowley, J. N., and J., L.: The Comparative Reactivity Method  
727 - a new tool to measure total OH reactivity in ambient air, *Atmos. Chem. Phys.*, 8, 2213-  
728 2227, doi: 10.5194/acp-8-2213-2008, 2008.
- 729 Sinha, V., Custer, T. G., Kluepfel, T., and Williams, J.: The effect of relative humidity  
730 on the detection of pyrrole by PTR-MS for OH reactivity measurements, *Int. J. Mass*  
731 *Spectrom.*, 282, 108-111, doi: 10.1016/j.ijms.2009.02.019, 2009.
- 732 Sinha, V., Williams, J., Lelieveld, J., Ruuskanen, T. M., Kalos, M. K., Patokoski, L.,  
733 Hellen, H., Hakola, H., Mogensen, D., Boy, M., Rinne, L., and M., K.: OH reactivity  
734 measurements within a boreal forest - evidence for unknown reactive emissions,  
735 *Environ. Sci. Technol.*, 44, 6614-6620, doi: 10.1021/es101780b, 2010.
- 736 Sinha, V., Williams, J., Diesch, J. M., Drewnick, F., Martinez, M., Harder, H., Regelin,  
737 E., Kubistin, D., Bozem, H., Hosaynali-Beygi, Z., Fischer, H., Andrés-Hernández, M.  
738 D., Kartal, D., Adame, J. A., and Lelieveld, J.: Constraints on instantaneous ozone  
739 production rates and regimes during DOMINO derived using in-situ OH reactivity  
740 measurements, *Atmos. Chem. Phys.*, 12, 7269-7283, doi: 10.5194/acp-12-7269-2012,



- 741 2012.
- 742 Stockwell, W. R., Kirchner, F., Kuhn, M., and Seefeld, S.: A new mechanism for  
743 regional atmospheric chemistry modeling, *J. Geophys. Res.-Atmos.*, 102, D22, 25847-  
744 25879, doi: 10.1029/97jd00849, 1997.
- 745 Stone, D., Whalley, L. K., and Heard, D. E.: Tropospheric OH and HO<sub>2</sub> radicals: field  
746 measurements and model comparisons, *Chem. Soc. Rev.*, 41, 6348-6404, doi:  
747 10.1039/c2cs35140d, 2012.
- 748 Tan, Z. F., Fuchs, H., Zhang, Y. H., et al., *Atmos. Chem. Phys.*, in preparation.
- 749 Wang, M., Zeng, L., Lu, S., Shao, M., Liu, X., Yu, X., Chen, W., Yuan, B., Zhang, Q.,  
750 Hu, M., and Zhang, Z.: Development and validation of a cryogen-free automatic gas  
751 chromatograph system (GC-MS/FID) for online measurements of volatile organic  
752 compounds, *Anal. Methods*, 6, 9424-9434, doi: 10.1039/c4ay01855a, 2014a.
- 753 Wang, M., Shao, M., Chen, W. T., Yuan, B., Lu, S. H., Zhang, Q., Zeng, L. M., Wang,  
754 Q.: A temporally and spatially resolved validation of emission inventories by  
755 measurements of ambient volatile organic compounds in Beijing, China. *Atmos. Chem.*  
756 *Phys.* 14, 5871-5891, doi: 10.5194/acp-14-5871-2014, 2014b.
- 757 Wang, M., Shao, M., Chen, W., Lu, S., Liu, Y., Yuan, B., Zhang, Q., Zhang, Q., Chang,  
758 C. C., Wang, B., Zeng, L., Hu, M., Yang, Y., and Li, Y.: Trends of non-methane  
759 hydrocarbons (NMHC) emissions in Beijing during 2002–2013, *Atmos. Chem. Phys.*,  
760 15, 1489-1502, doi: 10.5194/acp-15-1489-2015, 2015.
- 761 Wang, T., Ding, A., Gao, J., and Wu, W. S.: Strong ozone production in urban plumes  
762 from Beijing, China. *Geophys. Res. Lett.*, 33, L21806, doi: 10.1029/2006gl027689, 2006.
- 763 Whalley, L. K., Stone, D., Bandy, B., Dunmore, R., Hamilton, J. F., Hopkins, J., Lee, J.  
764 D., Lewis, A. C., and Heard, D. E.: Atmospheric OH reactivity in central London:  
765 observations, model predictions and estimates of in situ ozone production, *Atmos.*  
766 *Chem. Phys.*, 16, 2109-2122, doi: 10.5194/acp-16-2109-2016, 2016.
- 767 Williams, J.: Provoking the air, *Environ. Chem.*, 5, 317-319, doi:10.1071/en08048,  
768 2008.
- 769 Williams, J., and Brune, W. H.: A roadmap for OH reactivity research, *Atmos. Environ.*,  
770 106, 371-372, doi: 10.1016/j.atmosenv.2015.02.017, 2015.
- 771 Williams, J., Keßel, S. U., Nölscher, A. C., Yang, Y. D., Lee, Y. N., Yáñez-Serrano, A.  
772 M., Wolff, S., Kesselmeier, J., Klüpfel, T., Lelieveld, J., and Shao, M.: Opposite OH  
773 reactivity and ozone cycles in the Amazon rainforest and megacity Beijing: Subversion  
774 of biospheric oxidant control by anthropogenic emissions, *Atmos. Environ.*, 125, 112-



- 775 118, doi: 10.1016/j.atmosenv.2015.11.007, 2016.
- 776 Wu, Y., Yang, Y. D., Shao, M., and Lu, S. H.: Missing in total OH reactivity of VOCs  
777 from gasoline evaporation, Chinese. Chem. Lett., 26, 1246-1248, doi:  
778 10.1016/j.ccllet.2015.05.047, 2015.
- 779 Yang, Y., Shao, M., Wang, X., Nölscher, A. C., Kessel, S., Guenther, A., and Williams,  
780 J.: Towards a quantitative understanding of total OH reactivity: A review, Atmos.  
781 Environ., 134, 147-161, doi: 10.1016/j.atmosenv.2016.03.010, 2016.
- 782 Yoshino, A., Sadanaga, Y., Watanabe, K., Kato, S., Miyakawa, Y., Matsumoto, J., and  
783 Y., K.: Measurement of total OH reactivity by laser-induced pump and probe  
784 technique—comprehensive observations in the urban atmosphere of Tokyo, Atmos.  
785 Environ., 40, 7869-7881, doi: 10.1016/j.atmosenv.2006.07.023, 2006.
- 786 Yoshino, A., Nakashima, Y., Miyazaki, K., Kato, S., Suthawaree, J., Shimo, N.,  
787 Matsunaga, S., Chatani, S., Apel, E., Greenberg, J., Guenther, A., Ueno, H., Sasaki, H.,  
788 Hoshi, J., Yokota, H., Ishii, K., and Kajii, Y.: Air quality diagnosis from comprehensive  
789 observations of total OH reactivity and reactive trace species in urban central Tokyo,  
790 Atmos. Environ., 49, 51-59, doi: 10.1016/j.atmosenv.2011.12.029, 2012.
- 791 Yuan, B., Shao, M., de Gouw, J., Parrish, D. D., Lu, S., Wang, M., Zeng, L., Zhang, Q.,  
792 Song, Y., Zhang, J., and Hu, M.: Volatile organic compounds (VOCs) in urban air: How  
793 chemistry affects the interpretation of positive matrix factorization (PMF) analysis, J.  
794 Geophys. Res.-Atmos., 117, D24302, doi: 10.1029/2012jd018236, 2012.
- 795 Zhang, Q., Yuan, B., Shao, M., Wang, X., Lu, S., Lu, K., Wang, M., Chen, L., Chang,  
796 C. C., and Liu, S. C.: Variations of ground-level O<sub>3</sub> and its precursors in Beijing in  
797 summertime between 2005 and 2011, Atmos. Chem. Phys., 14, 6089-6101, doi:  
798 10.5194/acp-14-6089-2014, 2014.
- 799 Zhang, Y. H., Su, H., Zhong, L. J., Cheng, Y. F., Zeng, L. M., Wang, X. S., Xiang, Y.  
800 R., Wang, J. L., Gao, D. F., and Shao, M.: Regional ozone pollution and observation-  
801 based approach for analyzing ozone-precursor relationship during the PRIDE-  
802 PRD2004 campaign, Atmos. Environ., 42, 6203-6218, doi: 10.1016/j.atmosenv.2008.  
803 05.002, 2008.
- 804 Zhao, C., Wang, Y. H., Zeng, T.: East China Plains: a "Basin" of ozone pollution,  
805 Environ. Sci. Technol., 43, 1911-1915, doi: 10.1021/es8027764, 2009.
- 806 Zheng, J. Y., Shao, M., Che, W. W., Zhang, L. J., Zhong, L. J., Zhang, Y. H., Streets, D.,  
807 Speciated VOC emission inventory and spatial patterns of ozone formation potential in  
808 the Pearl River Delta, China. Environ. Sci. Technol. 43, 8580-8586, doi:



809 10.1021/es901688e, 2009.  
810 Zheng, J. Y., Zhong, L. J., Wang, T., Louie, P. K. K., Li, Z. C.: Ground-level ozone in  
811 the Pearl River Delta region: analysis of data from a recently established regional air  
812 quality monitoring network. Atmos. Environ. 44, 814-823, doi: 10.1016/j.atmosenv.  
813 2009.11.032, 2010.  
814 Zhao, W., Cohan, D. S., Henderson, B. H.: Slower ozone production in Houston, Texas  
815 following emission reductions: evidence from Texas Air Quality Studies in 2000 and  
816 2006. Atmos. Chem. Phys. 14, 2777-2788, doi: 10.5194/acp-14-2777-2014, 2014.  
817  
818  
819  
820  
821  
822  
823  
824  
825

Table 1 Total OH reactivity measurements in urban areas

Campaign	Site	Year	method	KOH(measured) (s <sup>-1</sup> ) <sup>a</sup>	KOH (calculated) (s <sup>-1</sup> if it is a value) <sup>b</sup>	Measured species <sup>c</sup>	Reference
SOS	Nashville, US	summer, 1999	LIF-flow tube	11.3	7.2	SFO	Kovacs et al., 2001; 2003;
PMTACS-NY 2001	NY, US	summer, 2001	LIF-flow tube	15-25	within 10%	SFO	Ren et al., 2003
PMTACS-NY 2004	NY, US	winter, 2004	LIF-flow tube	18-35	statistically lower	SF	Ren et al., 2006a
MCMA-2003	Mexico City, Mexico	spring, 2003	LIF-flow tube	10~120	30% less than	- <sup>d</sup>	Shirley et al., 2006
TexAQs	Houston, US	summer, 2000	LIF-flow tube	7~12	agree well	SFO	Mao et al., 2010
TRAMP2006	Houston, US	summer, 2006	LIF-flow tube	9-22	agree well	SFOB	Mao et al., 2010
	Tokyo, Japan	2003-2004	LP-LIF	10~100	30% less than	SFOB	Sadanaga et al., 2004; Yoshino et al., 2006
	Tokyo, Japan	summer, 2006	LP-LIF	10~55	30% less than	SFOB	Chatani et al., 2009
	Tokyo, Japan	spring, 2009	LP-LIF	10~35	22% less than	SFOB	Kato et al., 2011
	Tokyo, Japan	winter, 2007, autumn, 2009	LP-LIF	10~80	10~15 less than	SFOB	Yoshino et al., 2012





Table 1 Total OH reactivity measurements in urban areas (continued)

	Mainz, German	summer, 2005	CRM	10.4		-	Sinha et al., 2008
	Paris, France	winter, 2010	CRM	10~130	10~54% less than	SO	Dolgorouky et al., 2012
	London, England	summer, 2012	LP-LIF	10-116	20~40%	SFOB	Whalley et al., 2016
	Lille, France	autumn, 2012	CRM, LP-LIF	~70	Reasonable agreement	SFO	Hansen et al., 2015
	Dunkirk, France	summer, 2014	CRM	10-130		-	Michoud et al., 2015

- 827 a. For sources from different studies, the measured reactivity was presented as the averaged results, or ranges of diurnal variations, or the ranges of the whole campaign.  
828 b. For sources of different studies, the calculated reactivity was presented within an uncertainty range, as a percentage reduction or  $s^{-1}$  reduction.  
829 c. Measured species that have been used for the calculated reactivity (following Lou et al., 2010): S = inorganic compounds (CO, NO<sub>x</sub>, SO<sub>2</sub> etc) plus hydrocarbons  
830 (including isoprene); F = formaldehyde; O = OVOCs other than formaldehyde; B = BVOCs other than isoprene;  
831 d. “-” means a lack of information regarding what has been measured or how long it has been measured.

832  
833  
834  
835  
836  
837



838

Table2 Total OH reactivity measurements in suburban and surrounding areas

Campaign	Site	Year	method	$k_{OH}(\text{measured})$ ( $s^{-1}$ )	$k_{OH}(\text{calculated})$ ( $s^{-1}$ if it is a value)	Measured Species	Reference
PMTACS- NY2002	Central Pennsylvania, US	spring, 2002	LIF-flow tube	6.1	-	-	Ren et al., 2005
	Whiteface Mountain, US	summer, 2002	LIF-flow tube	5.6	within 10%	-	Ren et al., 2006b
TORCH-2	Weybourne, England	spring, 2004	LIF-flow tube	4.85	2.95	SFO	Ingham et al., 2009
CareBeijing-2006	Yufa, China	summer, 2006	LP-LIF	10-30	agree well	S	Lee et al., 2010 Lu et al., 2010; 2013
PRIDE-PRD	Backgarden, China	summer, 2006	LP-LIF	10~120	50% less than	S	Lou et al., 2010
DOMINO	El Arenosillo, Spain	winter, 2008	CRM	6.3~85	-	SF	Sinha et al., 2012

839

840

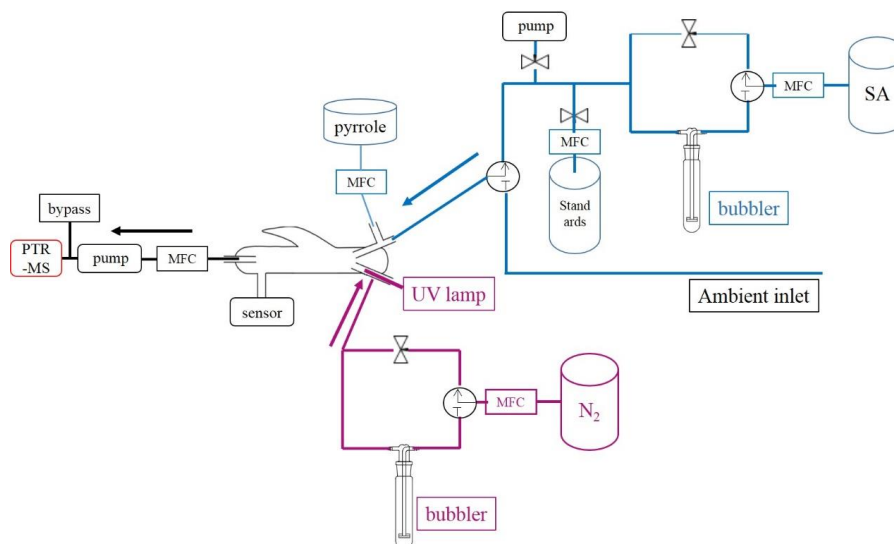
841

842

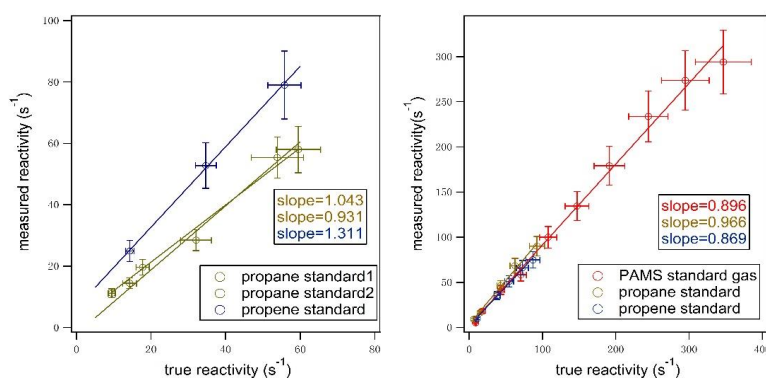
843



844



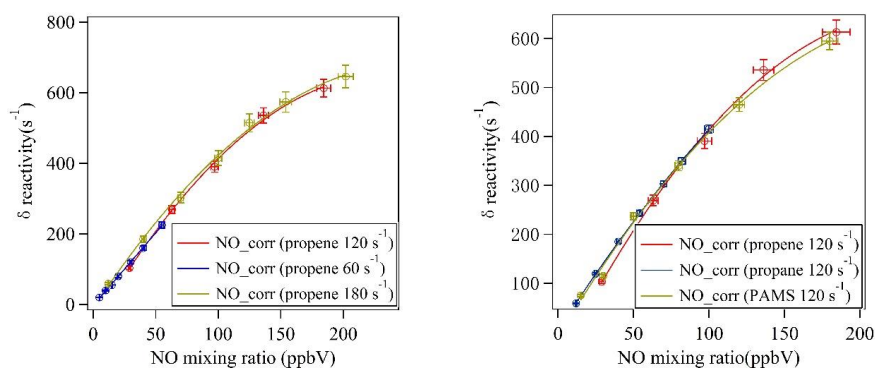
845 Fig 1 Schematic figures of CRM system in Beijing and Heshan observations.  
846 Blue color represents ambient air or synthetic air injection system, purple color  
847 represents OH generating system, black color represents the detection system.  
848 Pressure is measured by the sensor connected to the glass reaction.  
849



850  
851 Fig 2 OH reactivity calibration in Beijing (left) and Heshan (right).  
852 Left: Calibration in Beijing used two single standards: propane, propene;  
853 Right: Calibration in Heshan used three standards: propane, propene, mixed PAMS 56  
854 NMHCs.  
855 Error bars stand for estimated uncertainty on the measured and true reactivity.



856



857 Fig 3 NO-correction experiments and fitting curves in Heshan 2014.

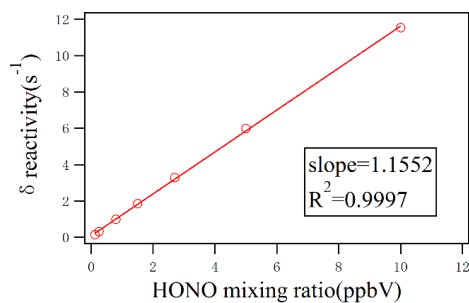
858 Left: NO-correction experiments with different mixing ratios of propene standard gas;

859 Right: NO-correction experiments with different standard gases at the same reactivity

860 level:  $120 \text{ s}^{-1}$ .

861 Error bars stand for estimated uncertainty on the NO mixing ratios and difference in

862 reactivity.

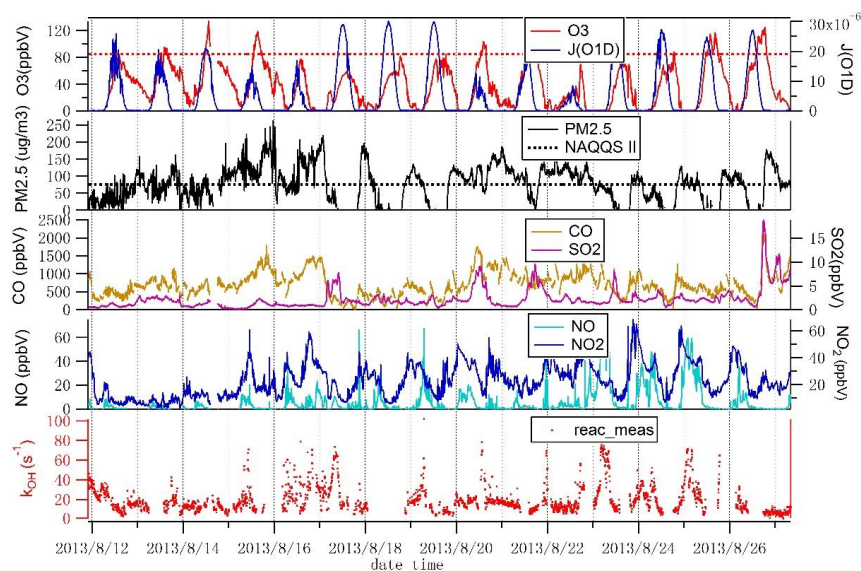


863

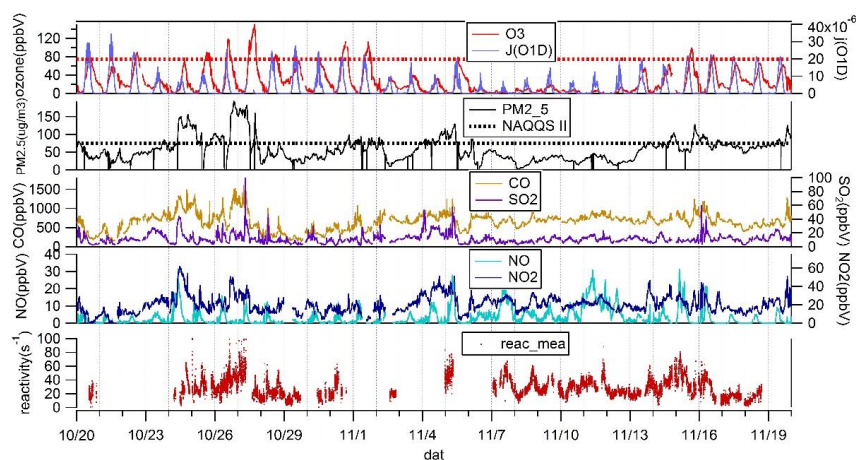
864 Fig 4 HONO-correction experiments and the fitting curve in Heshan 2014.

865

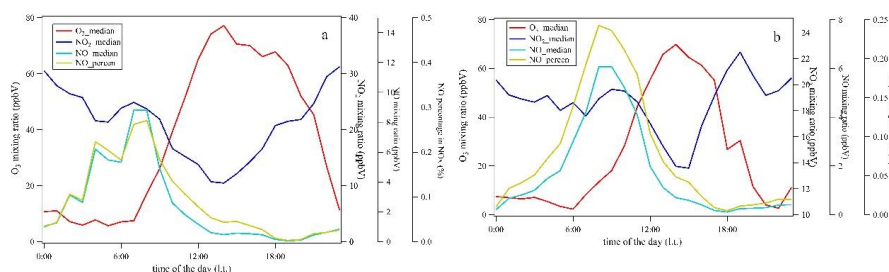
866



867  
868 Fig 5-a Time series of meteorological parameters and inorganic trace gases during  
869 August 2013 in Beijing.  
870 Red and black dashed lines are Grade II of National Ambient Air Quality Standard.  
871

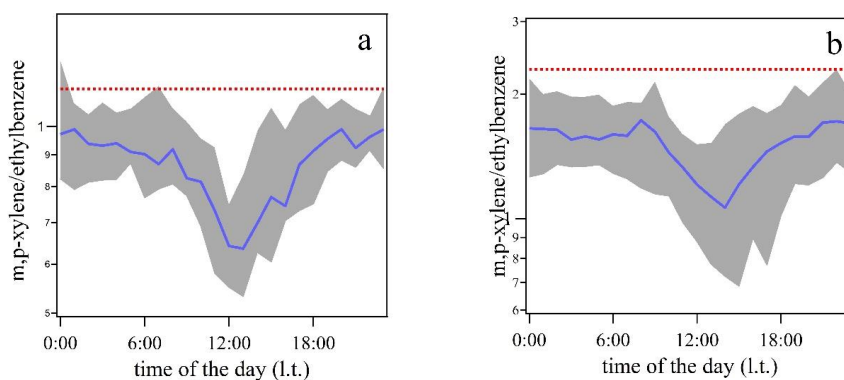


872  
873 Fig 5-b Time series of meteorological parameters and inorganic trace gases during  
874 October-November, 2014 in Heshan.  
875 Red and black dashed lines are Grade II of National Ambient Air Quality Standard.  
876  
877

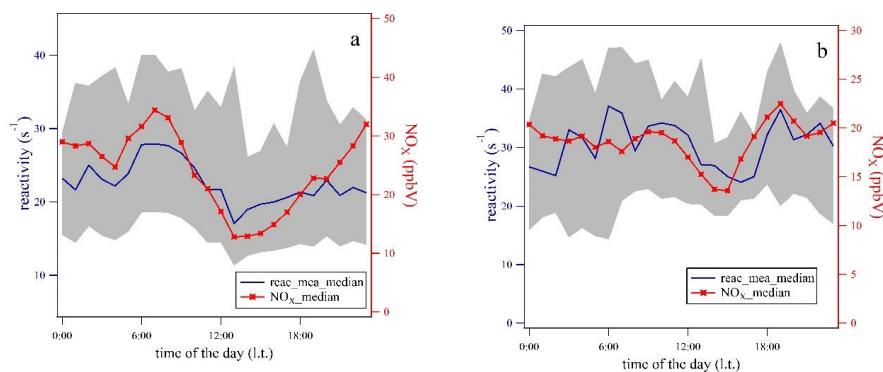


878 Fig 6 Diurnal variations of O<sub>3</sub>, NO, NO<sub>2</sub> and relative contribution of NO to NO<sub>x</sub>  
 879 in Beijing 2013 (a) and Heshan 2014 (b)  
 880

881

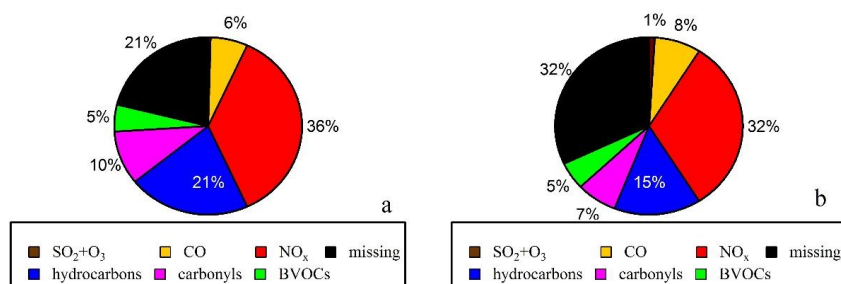


882 Fig 7 Ratios of m,p-xylene to ethylbenzene in Beijing 2013 (a) and Heshan 2014 (b)  
 883

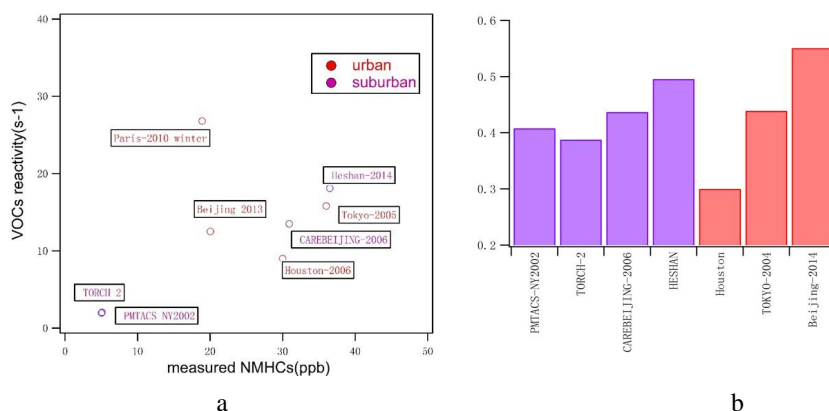


884 Fig 8 Diurnal variation of hourly median results of measured OH reactivity and NO<sub>x</sub>  
 885 mixing ratios in Beijing (a) and Heshan (b)  
 886  
 887

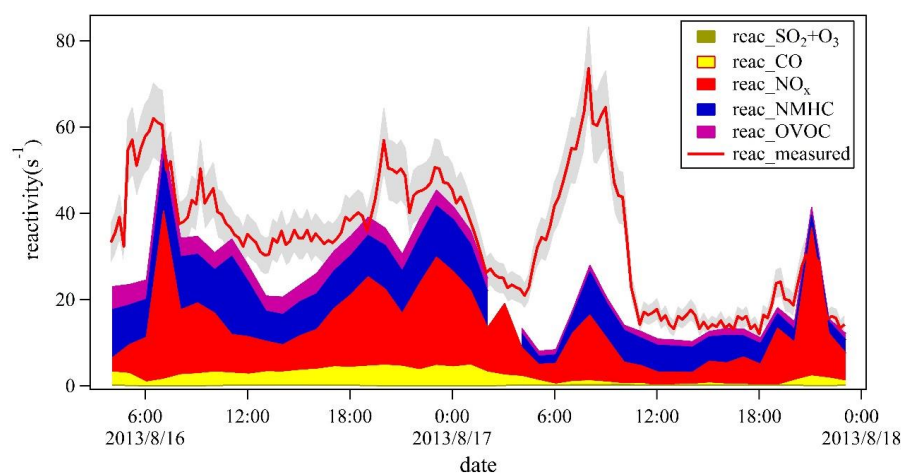
888

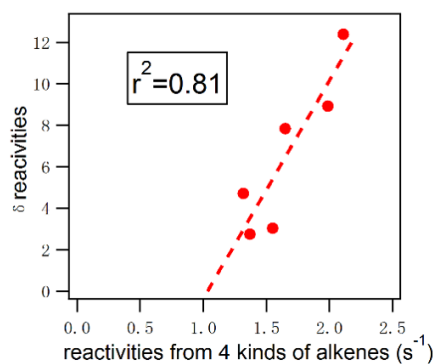


889 Fig 9 Composition of measured reactivity in Beijing (a) and Heshan (b)  
 890

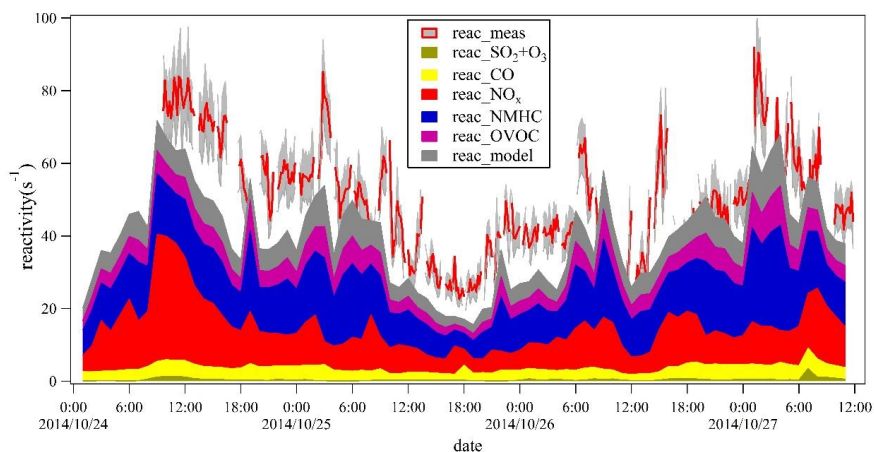


891  
 892  
 893 Fig 10 a: Comparison of VOCs reactivity and measured NMHCs in urban and suburban  
 894 observations.  
 895 b: Comparison of the ratio between VOCs reactivity and measured NMHCs in urban  
 896 and suburban observations  
 897

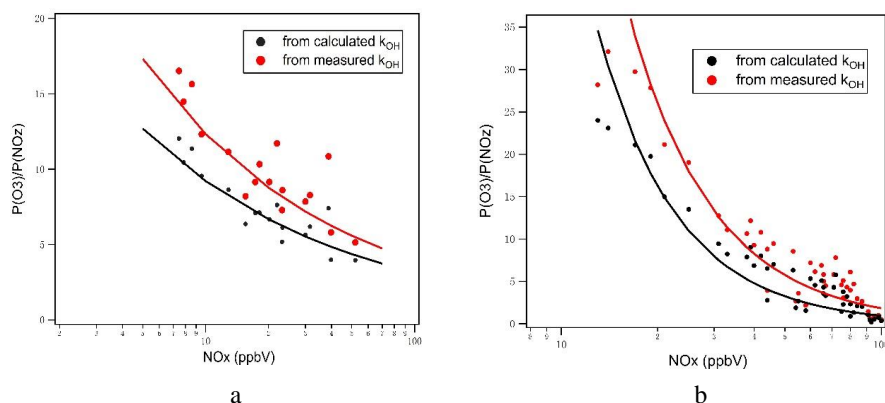




898  
899 Fig 11 Upper panel: Comparison between measured and calculated reactivity in Beijing  
900 August 16<sup>th</sup> to 18<sup>th</sup> 2013.  
901 Lower panel: Correlation between missing reactivity and reactivity assumed from  
902 branched-chain alkenes in diurnal patterns.  
903  
904



905 Fig 12 Comparison between measured reactivity and calculated reactivity as well as  
906 modelled reactivity in Heshan between October 24<sup>th</sup> and 27<sup>th</sup> 2014.  
907  
908  
909



910

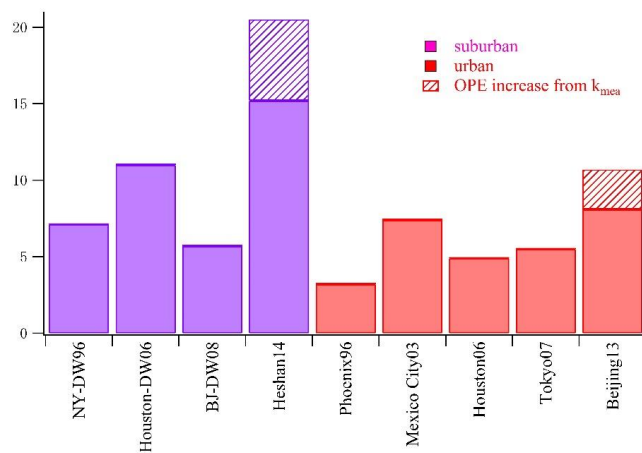
a

b

911 Fig 13 Comparison between OPE calculated from measured reactivity and calculated  
912 reactivity in Beijing (a) and Heshan (b).

913

914



915 Fig 14 Comparison between the OPE results in this study and other results from  
916 literatures. The comparison is made with the  $NO_x = 20$  ppbV. "DW" is in abbreviation  
917 of downwind.

918